Abstract of the thesis entitled

"Synthesis, Spectral Characterization and Structural Analysis of Transition Metal Complexes Containing Acyl Pyrazolone Ligands and their Applications"

To be submitted to

The Maharaja Sayajirao University of Baroda

For the Degree of

DOCTOR OF PHILOSOPHY

In Chemistry

By

Barad Sapnaben Vishnubhai

Under the Guidance of

Dr. R. N. Jadeja

Department of Chemistry,

Faculty of Science,

The Maharaja Sayajirao University of Baroda

VADODARA- 390002,

GUJARAT

October 2024

Abstract of the Thesis

To be submitted to The Maharaja Sayajirao University of Baroda for the degree of DOCTOR OF PHILOSOPHY in Chemistry

Title of the Thesis: "Synthesis, Spectral Characterization and Structural Analysis of Transition Metal Complexes Containing Acyl Pyrazolone Ligands and their Applications"

Name of the Student: Barad Sapnaben Vishnubhai

Name of the Supervisor: Dr. R. N. Jadeja

Department: Chemistry

Faculty: Science, The Maharaja Sayajirao University of Baroda

Registration number: FOS/2301

Date of registration: 27th October 2021

Barad Sapnaben Vishnubhai
Research Scholar

24/10/24

Dr. R. N. Jadeja
Research Guide

Department of Chemistry,
Faculty of Science,
The Maharaja Sayajirao University of Baroda
Vadodara.-390002. GUJARAT- INDIA.

Chapter 1: Introduction of transition metal complexes containing a derivative of pyrazolone ligands and their coordination chemistry

Chapter -**1** offers a brief overview of key advancements in transition metal chemistry, focusing on their coordination versatility, variable oxidation states, and roles in catalysis, biology, and materials science. It highlights significant discoveries in metal complexes' synthesis, characterization, and applications, emphasizing their biological importance.

Transition metal chemistry and its characteristics

Transition metals are highly valued for their exceptional characteristics, making them superior in numerous applications compared to other elements. For instance, Copper, a vital trace metal found in the form of Cu^{2+}, plays a significant role in metalloenzymes such as cytochrome oxidase, superoxide dismutase, and ascorbate oxidase and nickel (Ni) is involved in the enzyme urease. Metal ions are essential in pharmaceuticals and are also used as diagnostic agents. Given the unique properties of metals, their advantages in drug discovery should be further harnessed for the design of new pharmaceuticals. metal-based drugs are likely to play a crucial role in advancing drug development and enhancing the quality of life for patients.

Acylpyrazolone and application

Pyrazolone can be viewed as a derivative of pyrazole possessing an additional carbonyl (C=O) group. These compounds feature a 5-membered heterocyclic structure with two adjacent nitrogen atoms with an additional carbonyl (C=O) group. By 1959, Jensen and coworkers outlined a one-step synthesis method that involves acylating the C-4 position of the pyrazole ring in a basic dioxane solution with calcium hydroxide at reflux temperature (Jensen paper). class of β-diketones, where a pyrazole ring is integrated with a chelating functional group. Chelation by acylpyrazolonates is facilitated by a lower pKa value than those of conventional dicarbonyl ligands, leading to greater separation efficacy, and intense colours due to electronic transitions. acylpyrazolone ligands have been used for complexation with various transition metals.

A brief review: Work done on Cu(II) and Ni(II) complexes

This section provides a brief literature review of both recent and past research on transition metal complexes with acylpyrazolones. The four, five and six coordinated copper complexes and six coordinated Ni(II) have been synthesized. The synthesized copper complexes exhibited biological activity. The recent reviews by Marchetti and colleagues have explored the various applications of pyrazolone-based transition metal complexes, as well as the properties and uses of acylpyrazolone ligands and their corresponding transition metal complexes. Although Cu(II) complexes derived from pyrazolone derivatives are extensively researched for their biological effects,The first known compounds of Nickel(II) 4-aminoalkylidene-5-pyrazolone were found to be dihydrate octahedral paramagnetic with two unpaired electrons.

***In vitro* Anticancer activity**

This section provides information about how the copper acylpyrazolone complexes are important as an anticancer agent having fewer side effects than cisplatin. MTT assay, live dead assay, scratch assay and gene expression study are the part of *in vitro* cytotoxicity assay. MTT assay is a rapid colourimetric assay based on the tetrazolium salt MTT (3-(4,5-dimethylthiazol-2-yl)-2,5-diphenyl tetrazolium bromide), used to check the IC_{50} value of the compound against any cancer cell line. A promising method for investigating the behaviour of cancer cells is the scratch assay, which simulates wound healing to evaluate cell motility and proliferation. The Live/Dead assay is a common laboratory technique used in cell biology to assess cell viability, distinguishing between live and dead cells within a population using specific dyes. Gene expression study help understand the regulation of genes and their role in health, disease, and biological functions.

Aims and Objectives

The primary objective of this research is to synthesize acyl pyrazolone ligands and their complexes with copper and nickel transition metals. Comprehensive characterization was performed using techniques such as FTIR, NMR, TG-DTA, UV-VIS, Mass spectrometry, ESR, and CV, along with single-crystal

structure analysis. DFT and Hirshfeld studies were also conducted. Additionally, the *in vitro* anticancer activity of all the synthesized Cu(II) complexes have been assessed.

Chapter 2: Synthesis, Crystal Features and Characterization of a series of acylpyrazolone ligands: Computational analysis

Experimental work

Synthesis of ligands HL^{I} ,HL^{II} and HL^{III}

The synthetic pathway of HL^{I}, HL^{II} and HL^{III} ligands is depicted in **Fig.2.1.** Furthermore, ligands HL^{IV}, HL^{V}, HL^{VI}, HL^{VII}, HL^{VIII} and HL^{IX} were synthesized using a similar method and have been reported previously by our lab.

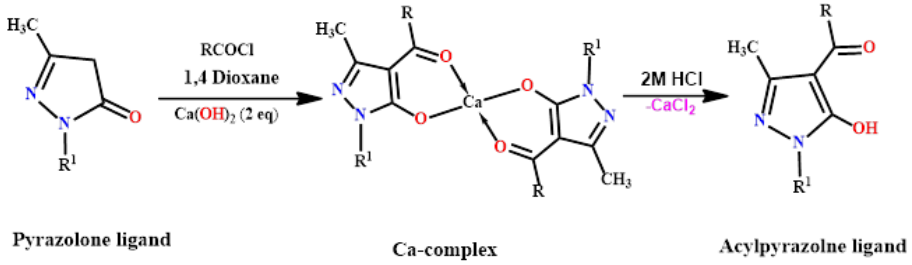

Fig.2.1. Synthetic route of ligands

> **R^1**= Phenyl, m-chloro phenyl and p-tolyl, **R**= 2,4-dichlorobenzoyl chloride (**HL^{I}, HL^{II} and HL^{III}**), **R**= 4-chlorobenzoyl chloride (**HL^{IV}, HL^{V} and HL^{VI}**), **R**= 3,5-dimethyl and 4-nitro benzoyl chloride (**HL^{VII}, HL^{VIII} and HL^{IX}**) ligands

HL^{I} ligand: Light orange, yield:85%, M.P: 128°C, **Molecular formula:** $C_{17}H_{12}Cl_2N_2O_2$, **M.W:** 347.20, **Elemental analysis**: C (Exp. 59.95%, Calc. 58.81%); H (Exp. 3.90%, Calc. 3.48%); N (Exp. 8.10%, Calc. 8.07%), **FTIR (KBr, cm^{-1}):** ν(C=O) of pyrazolone; (1627), ν(C=O) of 2,4 dichloro benzoyl, **NMR: ^{1}H NMR δ-ppm (400 MHz, $CDCl_3$):** 2.195 (s, 3H, CH_3(pyz)), 7.3–7.8 (m, Ar-H of HL^{I} ligand).

HL^{II} ligand: Brownish crystals, **yield:**86%, **M.P**: 135°C, **Molecular formula:** $C_{17}H_{11}Cl_3N_2O_2$, **M.W:** 381.64, **Elemental analysis**: C (Exp. 54.10%, Calc. 53.50%); H (Exp. 3.05%, Calc. 2.91%); N (Exp. 7.50%, Calc. 7.34%), **FTIR (KBr, cm^{-1}):** ν(C=O) of pyrazolone; (1594), ν(C=O) of 2,4 dichloro benzoyl; (1550), **^{1}H NMR δ-ppm (400 MHz, CDCl3**): d ppm:1.89 (s, 3H, Pyrazolone C-CH3), 7.3–7.9 (m, Ar-H of HL^{II} ligand).

HL^{III} ligand: Orange-brown: yield:86%, **M.P**: 131°C, **Molecular formula:** $C_{18}H_{14}Cl_2N_2O_2$, **M.W:** 361.22, **Elemental analysis**: C (Exp. 60.12%, Calc. 59.85%); H (Exp. 4.10%, Calc. 3.91%); N (Exp. 7.85%, Calc. 7.76%), **FTIR (KBr, cm^{-1}):** ν(C=O) of pyrazolone; (1668), ν(C=O) of 2,4 dichloro benzoyl; (1585), **^{1}H NMR δ-ppm (400 MHz, $CDCl_3$)**: d ppm:1.94 (s, 3H, Pyrazolone C-CH3), 7.4–7.7 (m, Aromatic-H of HL^{III} ligand).

Results and discussion

^{1}H NMR and FTIR spectral studies

The ^{1}H NMR spectra of the synthesized HL^{I}, HL^{II}, HL^{III} ligands in $CDCl_3$ are in good agreement with the proposed structure. The infrared spectra (4000-400 cm^{-1} KBr discs) of prepared ligands were done on model Brucker alpha.

Single crystal X-ray diffraction study

Crystal structure of HL^{I}, HL^{II}, HL^{III} ligands were obtained in the form of keto, enol and keto having form '**Triclinic'** crystal system with *P*-1 space group, '**Monoclinic'** crystal system with $P2_{1/n}$ space group**, 'Triclinic'** crystal system with *P*-1 space group respectively.

DFT based computational analysis and Hirshfeld analysis

B3LYP/6-31G level basis set was used to compute the optimized geometry of ligands with energy value -49.934 keV, -62.440 keV and -51.004 keV for HL^{I}, HL^{II} and HL^{III} ligands accordingly.The distribution of frontier orbital can be used to analyse active sites and reactivity. To learn more about how molecules interact

in crystal formations, we have employed Hirshfeld surfaces analysis. This study has provided a thorough description of the immediate surroundings of the molecule. The crystal explorer 17.5 programme was utilised to visualise and investigate an intermolecular interactions and donor-acceptor interaction sites in this analysis. The red and blue patches show how π … π stacking interaction in the molecule. Energy calculations were carried out for a 3.8 Å cluster surrounding the chosen HS of ligands. The fast [HF/3-21G] model of the Crystal Explorer 17.5 program was utilised to calculate the interaction energy data.

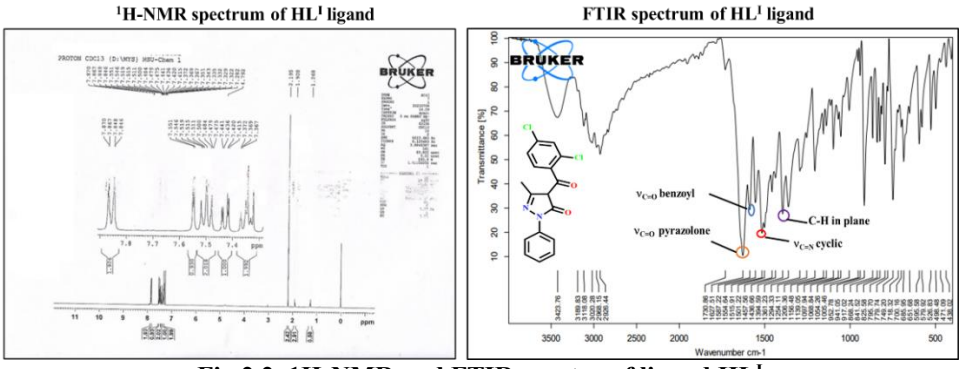

Fig.2.2. 1H-NMR and FTIR spectra of ligand HL^{I}

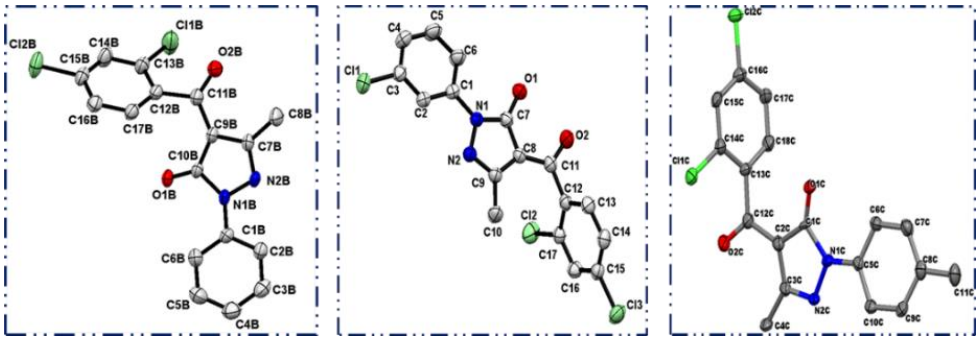

Fig.2.3. ORTEP diagram of HL^{I}, HL^{II}, HL^{III} ligands

Table 2.1. Crystal data and refinement parameters of ligands HL^{I}, HL^{II} and HL^{III}

CODE	HL^{I} ligand	HL^{II} ligand	HL^{III} ligand
Unit cell dimension	a = 11.5502(3) Å b = 11.5976(3) Å c = 12.1851(3) Å α= 93.586(2)° β= 90.901(2)° γ= 105.568(2)°	a = 7.44180(10) Å b = 11.3843(2) Å c= 19.8633(4) Å α,= 90° β= 97.5520(10)° γ = 90°	a = 12.1180(3) Å b = 12.3703(4) Å c = 12.5275(5) Å α= 62.609(4)° β= 87.115(3)° γ= 87.752(3)°

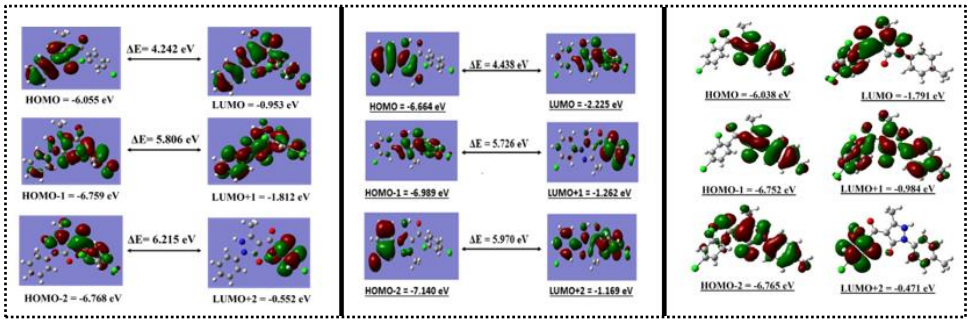

Fig.2.4. HOMO-LUMO molecular diagram of HL^{I}, HL^{II}, HL^{III} ligands

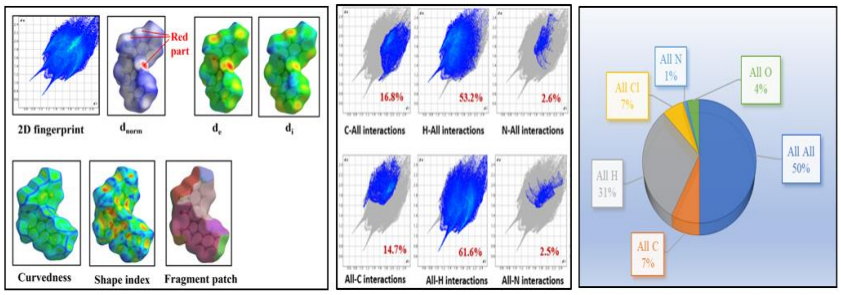

Fig.2.5. Hirshfeld diagram of HL^{I} ligand

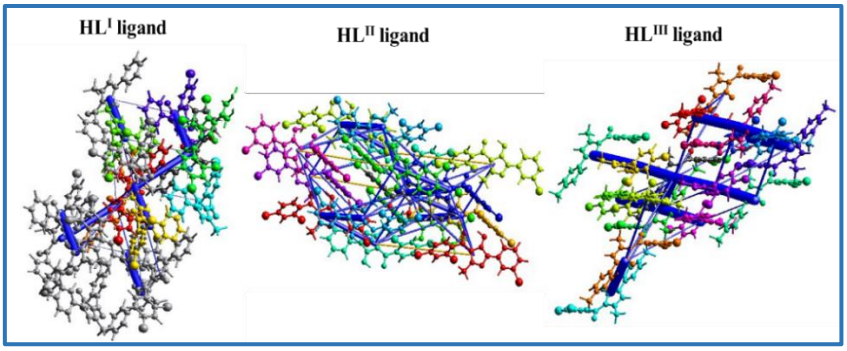

Fig.2.6. Energy frameworks of ligands based on Total energy

Conclusions

Three acylpyrazolone ligands were synthesized and characterized. Structural elucidation using FTIR spectral analysis shows significant vibrations. The single crystal data are largely used to examine their structure, geometry, composition, surface interactions, and lattice energy. The Hirshfeld surface analysis was also carried out to identify the crystal strength through interaction energies and intermolecular non-covalent surface interactions in the ligand.

Chapter 3; Synthesis, Characterization and Structural assessment of biologically active Square pyramidal Cu(II) acylpyrazolone complexes: DFT, Hirshfeld analysis

Part (a): Square pyramidal Cu(II) acylpyrazolone complexes: Synthesis, characterization, crystal structure, DFT and Hirshfeld analysis; *in-vitro* anti-cancer evaluation

Experimental work

Synthetic route of complex-1 & complex-2

A hot methanolic solution of 1 eq copper sulphate and 2 eq HL^{II} and HL^{IX} ligands were refluxed in two different round bottom flasks at 70-80°C for 3-4 hours. After refluxing, the solutions were filtered, and the products were washed using hot methanol and dried and recrystallized from hot DMF and DMSO solvents, respectively. Thick green plate-shaped X-ray quality single crystals of complex-**1** and complex-**2** were obtained after a few days. Both complexes are stable at room temperature. DMF and DMSO solvents occupy the apical position (5th coordination site) in complex-**1** and complex-**2**, respectively as confirmed by single-crystal X-ray analysis. The synthetic route of complex-**1** and complex-**2** are demonstrated in **Fig.3a.1**.

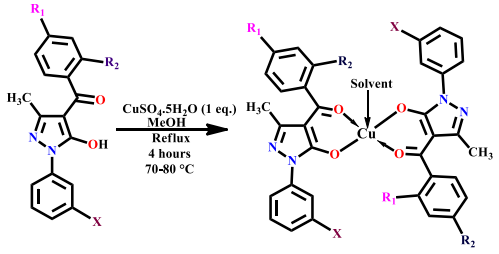

Complex-1: R_1= Cl, R_2= Cl, X= Cl, **Complex-2**: R_1= NO_2, R_2= H, X =

Fig.3a.1. Synthetic route of complex-1 and complex-2

Complex-1: **Colour**: Green, yield: 82%, M.P:> 200°C, Molecular formula: $C_{34}H_{20}CuCl_6N_4O_4$.DMF, **M.W:** 824.811, **Elemental analysis**: C (Exp. 53.10%, Calc.: 52.69%); H (Exp. 2.90%, Calc. 2.80%); N (Exp. 8.21%, Calc. 7.21%); Cu (Exp. 8.10%, Calc. 7.08%), **Molar conductance (10^{-3} M DMF):** 2.18 $ohm^{-1}cm^2mol^{-1}$.
Complex-2: **Colour**: Green, yield: 83%, M.P.: >200°C, Molecular formula: $C_{34}H_{24}CuN_6O_8$.DMSO, **M.W:** 708.136, **Elemental analysis**: C (Exp. 56.55%, Calc. 55.53%); H (Exp. 4.50%, Calc. 4.03%); N (Exp. 10.80%, Calc. 10.50%); S (Exp. 2.80%, Calc. 2.77%); Cu (Exp. 8.05%, Calc. 7.94 %), **Molar conductance (10^{-3} M DMF):** 3.90 $ohm^{-1}cm^2mol^{-1}$.

Results and discussion

FTIR spectral studies

FTIR reveals critical information about the functional groups and molecular structures within the compound by analyzing how a sample absorbs infrared light. Theoretical vibrations can be used to investigate the changes which occur during complexation. Theoretical IR frequencies were obtained using DFT calculations after the complete optimization.

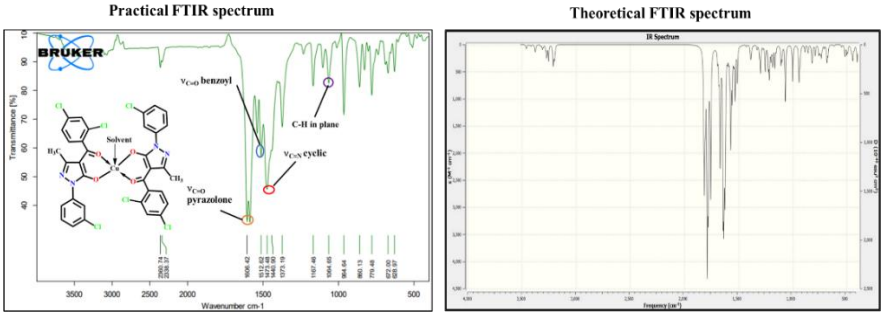

Fig.3a.2. FTIR spectra of complex-1

Table 3a.1. FTIR spectral data of ligands, complexes 1 and 2

Code	HL^{II} ligand	Complex-1	HL^{VI} ligand	Complex-2
ν(C=O) of benzoyl chloride	1550	1512	1519	1567
ν(C=O) of Pyrazolone	1594	1606	1622	1604
Cyclic ν(C=N)	1482	1473	1393	1380
C–H in plane deformation	1062	1064	1210	1244
ν_{M-O}	-	508	-	519

Thermogravimetric analysis

Three-step decomposition of 5 Co-ordinated complex-1 can be examined through the TGA analysis. Degradation of both the ligands can be observed at the range of 280-500°C.

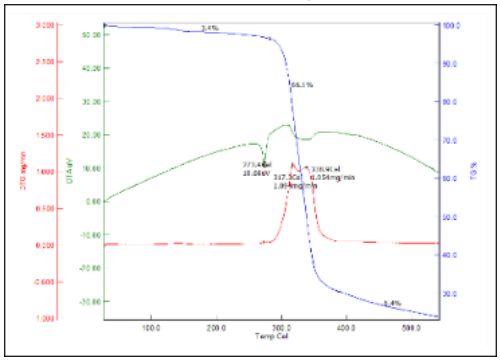

Fig.3a.3. TG-DTA plot of complex-1

Single crystal X-ray diffraction study

The molecular crystal structure of both copper complexes appeared as green-coloured, thick plate-shaped crystals. The geometry of both complexes is square pyramidal (penta-coordinated). Complex-**1** crystallizes in the '**Triclinic crystal system**' with the ***P*-1** space group and contains only an inversion centre as its symmetry element. complex-**2** has a '**Monoclinic crystal system**' with the $P2_{1/c}$ space group. This space group features a primitive lattice, a 2-fold screw axis along the b-axis and a c-glide plane.

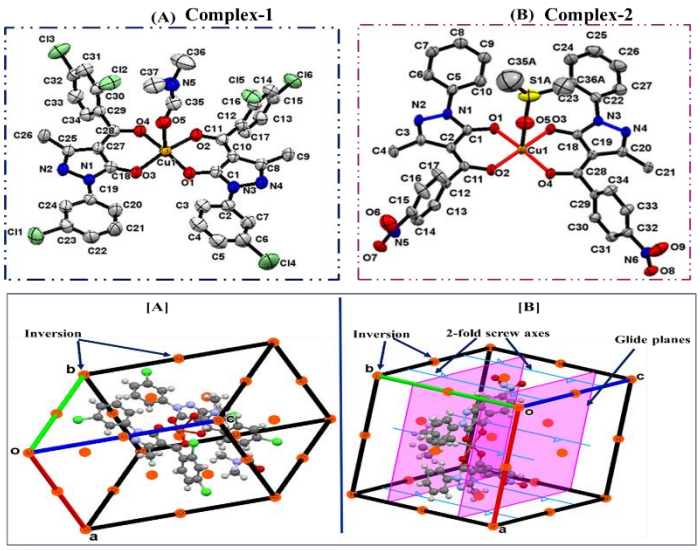

Fig.3a.4. ORTEP view and symmetry elements of [Cu(HL^{II})$_2$DMF] complex-1 and [Cu(HL^{IX})$_2$DMSO] complex-2

Computational analysis employing DFT

The B3LYP/6-31G level basis set was used to compute the optimized geometry with energy value -182.454 keV for complex-1. The B3LYP/ LANL2DZ level basis set was used to compute the geometry of complex-2 with a -125.564 keV energy value. Frontier orbitals have been studied because they are essential for determining chemical stability, energy value, and chemical behaviour.

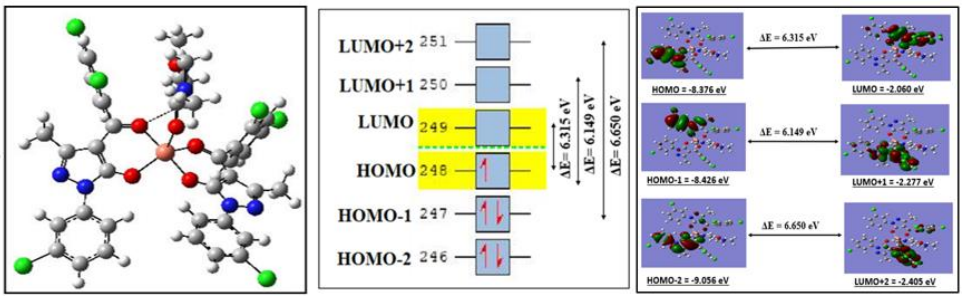

Fig.3a.5. DFT optimized structure and HOMO-LUMO orbital of complex-1

Table 3a.2. Global parameters of complex-1 and complex-2

Properties	Mathematical Formula	[Cu(HL^{II})$_2$DMF]	[Cu(HL^{IX})$_2$DMSO]
Ionization potential (IP)	IP = -E_{HOMO}	8.376	5.963
Chemical Potential (μ)	μ = 1/2 (E_{HOMO} + E_{LUMO})	-5.21	-4.501

Electronic spectral analysis, ESR analysis

UV-visible absorption spectra of both complexes were taken in DMSO solvent up to 950 nm (10526 cm^{-1}). A complex-**1** exhibited a sharp transition at 277 nm (36101cm^{-1}) whereas a complex-**2** exhibited n-π* transitions at 363 nm (27548 cm^{-1}) and π-π* transitions at 280 nm (35714 cm^{-1}) within the ultraviolet range due to intra-ligand charge transfer (ILCT) transitions. Additionally, the broad bands are observed at 800 nm (12500 cm^{-1}) and 768 nm (13020 cm^{-1}) in complex-**1** and complex-**2**, respectively. in the visible spectrum is attributed to a d-d transition. These transitions can be assigned to the $d_{x^2-y^2} \rightarrow d_{xz}$, d_{yz} and $d_{x^2-y^2} \rightarrow d_{z^2}$ transition. The ESR spectral analysis was carried out through ESR JEOL analysis in a Powder state at RT with tetracyanoethylene (TCNE) as a marker (g = 2.00277). Cu(II) exhibit four lines which can be seen from the graph. In this analysis $g_{\parallel (2.361)} > g_{\perp (2.050)} > 2.0023$ which suggests the ground state results from $dx^2\text{-}y^2$ orbital.

Electro-chemical analysis (CV)

The redox behaviour of both complexes was studied through the cyclic voltammetry (CV) technique. The diagrams show two oxidation and two reduction peaks. The value of ΔEp_1 is 0.5955 V and 0.3912 V for

complex-**1** while, ΔEp_2 is 1.6433 V and 1.5650 V for complex-**2**, respectively for each redox couple. The nature of the graphs is quasi-reversible.

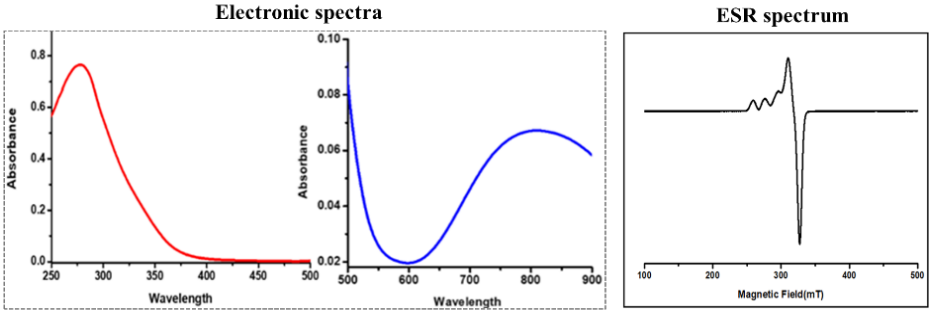

Fig.3a.6. Electronic spectra and ESR spectrum in powder form at RT of complex-1

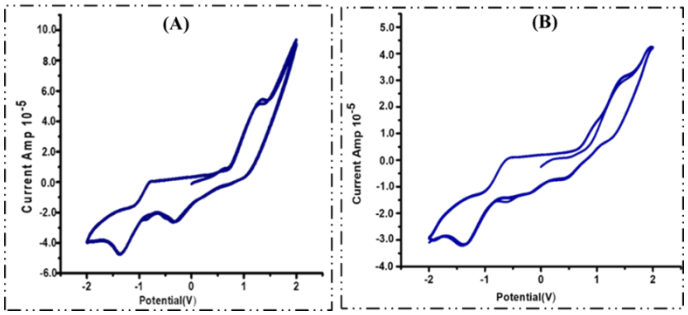

Fig.3a.7. Cyclic voltammograms of (A) complex-1 and (B) complex-2 in DMSO solution using 0.1 M TBAP at scan rate 100 mV and 50 mV, respectively

Hirshfeld surface analysis

This study has provided a thorough description of an immediate surroundings of the molecule. The Crystal Explorer 17.5 programme was utilised to visualise and investigate intermolecular interactions and donor-acceptor interaction sites in this analysis. The red and blue patches show how π … π stacking interacts in the molecule.

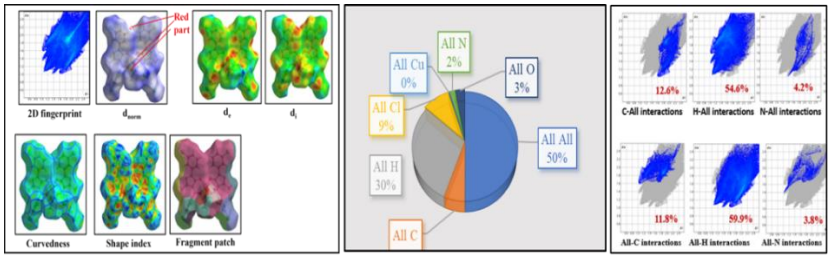

Fig.3a.8. Molecular Hirshfeld & 2d fingerprint plot of complex-1

***In vitro* Anticancer activity**

The anticancer efficacy of both complexes was evaluated using a cytotoxicity assay, revealing a significant level of cytotoxic activity. Both complexes were tested against three different cancer cell lines: NCI-H23 (lung cancer), HepG2 (liver cancer), and SH-SY5Y (neuroblastoma). The IC_{50} value represents the concentration at which 50% inhibition of cell growth occurs.

Table 3a.11. Percent inhibition (IC_{50} values) of complex-1 and complex-2 against NCI-H23, SH-SY5Y and HepG2 cancer cells

Percent inhibition (IC_{50} values)			
Compounds	**Complex-1**	**Complex-2**	**Cisplatin**
NCI-H23	14.3 µM	-	17.65 µM
SH-SY5Y	7.2 µM	36.74 µM	44.94 µM
HepG2	7.1 µM	-	-

Cell death analysis & Scratch assay

Cell death analysis provides a count of both live and dead cells using calcein and EthD-1 dyes which is responsible for green fluorescence (indicates live cells) and red fluorescence (indicates dead cells) respectively. Remarkable cell death could be observed as shown by predominant red fluorescence. Scratch assay is a straightforward and economical method to study cell migration in vitro. It has been examined at three different times interval : at 0 h, 24 h and 48 h. At 24 h to determine the rate of cell migration. At 24hr nearly 41% of the wound closer was seen in the control medium while 29% can be observed in treated condition.

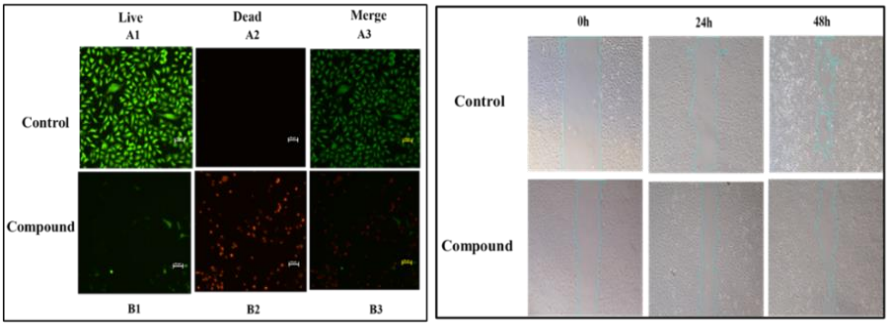

Fig.3a.9. (A) Dual staining (live/dead assay) of NCI-H23 cells exposed to complex-1, (B) Scratch assay

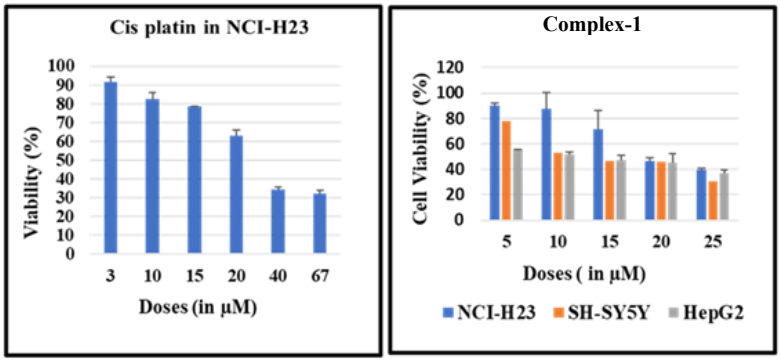

Fig.3.10. Percent viability of NCI-H23 Cells exposed to indicated doses of Cisplatin and complex-1

Conclusion

The present research demonstrates the pharmacological potency of pyrazolone derivatives and their Copper(II) metal complexes. Two complexes, complex-**1** and complex-**2** were synthesized and thoroughly characterized using a range of analytical techniques. Single-crystal X-ray diffraction analysis confirmed the square pyramidal geometry of both complexes. The data revealed the binding sites, where four oxygen atoms from the ligands coordinated to the central Cu(II) metal at equatorial positions, while an oxygen atom from DMF and DMSO coordinated at the axial position in complex-**1** and complex-**2**, respectively. ESR study suggested the paramagnetic behaviour of a complex. Redox behaviour can be understood by CV. *In vitro* anticancer activity suggests the encouraging application of both complexes.

Part (b): Acylpyrazolone based square pyramidal Cu(II) complexes: Synthesis, structural characterization, DFT and antiproliferative properties

Experimental work

Synthetic route of complex-3 & complex-4

Both copper complexes, complex-**3** and complex-**4**, were prepared using the same procedure described in Chapter **3a**

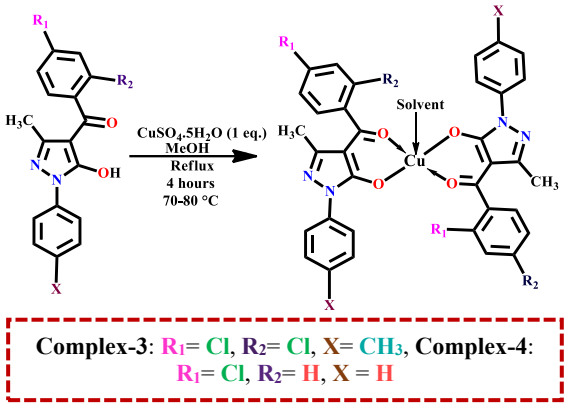

Fig.3b.1. Synthetic route of complex-3 and complex-4

Complex-3: **Colour**: Yellowish green, yield: 78%, M.P:> 200°C, Molecular formula: $C_{36}H_{26}CuCl_4N_4O_4$.DMF **Crystal:** Dark green prism-shaped, **M.W:** 783.974, **Elemental analysis**: C (Exp. 54.97%, Calc.: 54.65%); H (Exp. 3.98%, Calc. 3.88%); N (Exp. 8.90%, Calc. 8.71%); Cu (Exp. 8.00%, Calc.7.98 %), **Molar conductance (10^{-3} M DMF):** 3.27 $ohm^{-1}cm^2mol^{-1}$.

Complex-4: **Colour**: Green, yield: 76%, M.P:> 200°C, Molecular formula: $C_{34}H_{24}CuCl_2N_4O_4$.DMSO, **Crystal:** Thick green plate-shaped, **M.W:** 687.031, **Elemental analysis**: C (Exp. 56.79%, Calc.: 56.51%); H (Exp. 4.10%, Calc. 3.95%); N (Exp. 7.56%, Calc. 7.32%); Cu (Exp. 8.04%, Calc. 8.01%), **Molar conductance (10^{-3} M DMF):** 3.87 $ohm^{-1}cm^2mol^{-1}$.

Results and discussion

FTIR spectral studies

FTIR is an instrumental technique which details the molecular properties of the synthesized copper complexes. During complexation, the charge from the O-atom of the C=O group in pyrazolone is transferred to the metal ion, which strengthens the M-O bond and weakens the C=O bond, leading to an increase in the bond length of the pyrazolone C=O bond. Theoretical vibrations can be used to investigate the changes which occur during complexation. Theoretical IR frequencies were obtained using DFT calculations after the complete optimization.

Table 3b.1. FTIR spectral data of respective ligands, complexe-3 and complex-4

Code	HL^{III} ligand	Complex-3	HL^{IV} ligand	Complex-4
ν(C=O) of benzoyl chloride	1585	1505	1587	1575
ν(C=O) of Pyrazolone	1668	1598	1619	1597
Cyclic ν(C=N)	1472	1363	1557	1479
C–H in plane deformation	1253	1161	1213	1162
ν_{M-O}	-	508	-	490

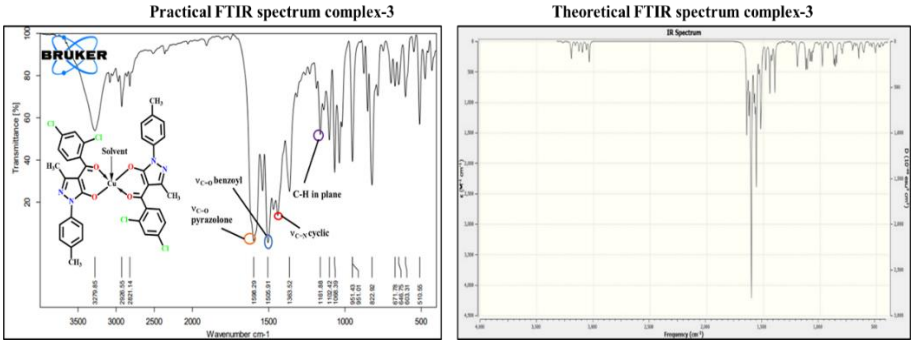

Fig.3b.2. FTIR spectra of complex-3

Thermogravimetric analysis

TGA, or thermogravimetric analysis, explains how a material's mass changes with temperature. The aforementioned methodology can be used to evaluate the three-step decomposition of complex-**3** and complex-**4.**

Single crystal X-ray diffraction study

The complex-**3** and complex-**4** were recrystallized in DMF and DMSO solvents, respectively. Thick green crystals of both complexes were obtained. The geometry of the synthesized complexes was determined to be square pyramidal (penta-coordinated), where four oxygen atoms from two ligands occupy the equatorial positions and the fifth position is coordinated by an oxygen atom from a DMF molecule (in complex-**3**) and a DMSO molecule (in complex-**4**).

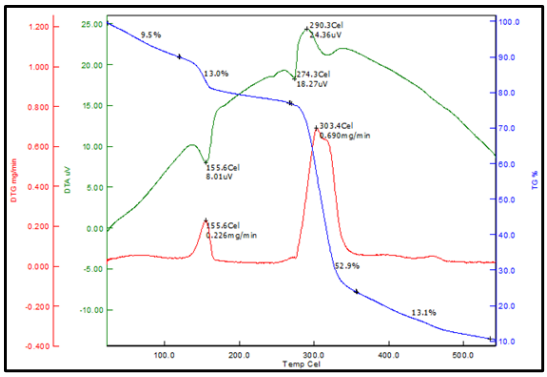

Fig.3b.3. TG-DTA plot of complex-3

Table 3b.2. Refinement parameters of complex-3 and complex-4

CODE	[Cu(HL^{III})$_2$DMF] Complex-3	[Cu(HL^{IV})$_2$DMSO] Complex-4
Crystal system	Monoclinic	Monoclinic
Space group	$P2_1$/n	$P2_1$/c
Unit cell dimension	a= 13.9750(17) Å b= 6.8795(9) Å c= 39.669(5) Å	a= 14.415(4) Å b= 16.478(4) Å c= 14.620(4) Å
	α,γ = 90° β=93.355(6)°	α,γ = 90° β= 101.557(8)°

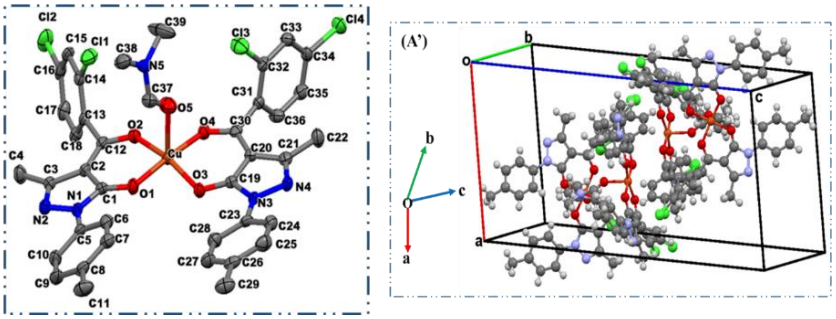

Fig.3b.4. ORTEP view and crystal packing of [Cu(HL^{III})$_2$DMF] complex-3

DFT based computational analysis

The geometries were computed using B3LYP/LANL2DZ and B3LYP/6-31G levels for both complexes. The optimization energy of [Cu(HL^{III})$_2$(DMF)] and [Cu(HL^{IV})$_2$(DMSO)] complexes is -65.6225 keV and -60.4222 keV respectively when computed at B3LYP/LANL2DZ. The observed energy is -139.7153 keV and -134.5150 keV while utilizing B3LYP/6-31G basis set. For a variety of chemical interactions, the HOMO-LUMO energies are essential.

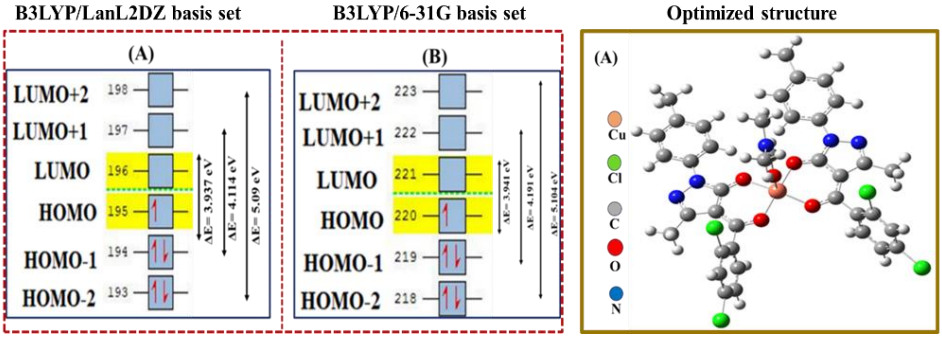

Fig.3b.5. HOMO-LUMO energy diagram and DFT optimized structure of complex-3

Table 3b.3. Global parameters (at LanL2DZbasis set) of complex-3 and complex-4

Properties	Mathematical Formula	$[Cu(HL^{III})_2DMF]$	$[Cu(HL^{IV})_2DMSO]$
Ionization potential (IP)	$IP = -E_{HOMO}$	5.794	5.950
Chemical Potential (μ)	$\mu = 1/2 (E_{HOMO} + E_{LUMO})$	-3.825	-4.027

Electronic spectral analysis, ESR analysis

The crystal sample underwent UV-visible absorption investigations up to 950 nm to determine the energy gap of copper complexes. DMSO solvent was used for the analysis. The absorbance of a transition can be categorised as the $d_{x^2-y^2} \rightarrow d_{xz}$, d_{yz}, and $d_{x^2-y^2} \rightarrow d_{z^2}$ it is because of the Jahn-Teller distortion in the complexes. The specific transition follows the $^2E_g \rightarrow {}^2T_{2g}$ transition. The specific transition follows the $^2E_g \rightarrow {}^2T_{2g}$ transition. Which interpreted as a Square Pyramidal geometry of both complexes.

Complex-3: d-d transition (768 nm), Molar absorbance (ε): 89.1 M^{-1} cm^{-1}

Complex-4: d-d transition (751 nm) Molar absorbance (ε): 57.1 M^{-1} cm^{-1}

To explain the magnetic behaviour of the copper complexes ESR analysis was conducted. Tetracyanoethylene (TCNE) was used as a marker (g = 2.00277) during the ESR JEOL analysis in the powder state at RT at in the solution state at LNT. The graphs show four lines that represent Cu(II). The value of $g_{\|}$ at RT is 2.545 and at LNT is found to be 2.353 for complex-**3.**

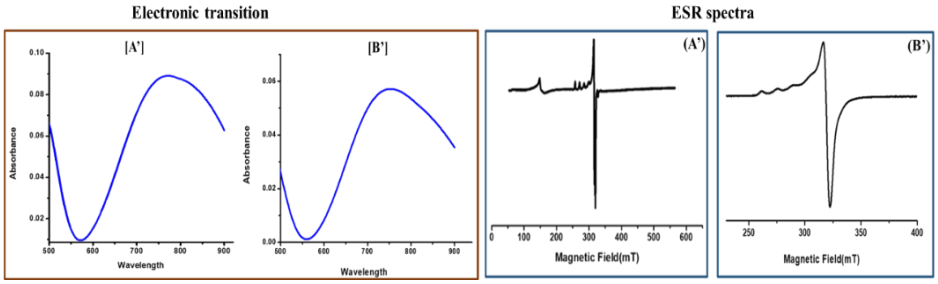

Fig.3b.6. Electronic spectra and ESR spectra in solution stat at LNT of (A') complex-3 & (B') complex-4

Hirshfeld surface area analysis &2d fingerprint plots

CrystalExplorer17.5 software was used to carry out the Hirshfeld surface analysis and create the 2D fingerprint plots of the molecules to illustrate the structural relationships of the crystal structures in this group of closely related compounds. Plotting the Hirshfeld surface (HS) using several characteristics, such as normalised distances (dnorm), de, di, shape index, curvedness, fragment patch etc, which gives an idea about the interaction and hydrogen bonding.

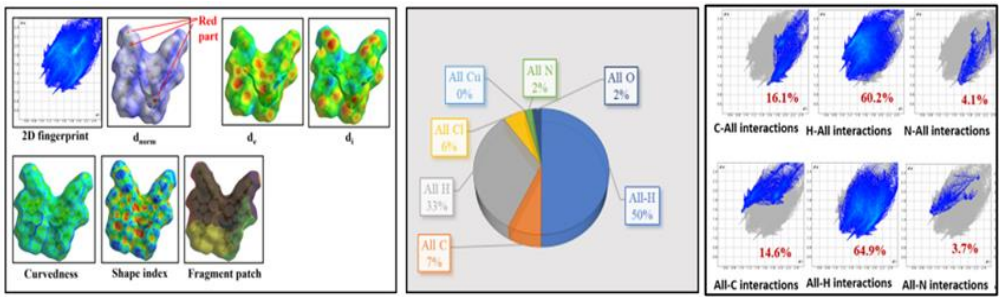

Fig.3b.7. Molecular Hirshfeld & 2d fingerprint plots of complex-3

Cytotoxicity assay

In vitro anticancer activity of a complex-2 has been done against NCI-H23, SH-SY5Y and HepG2 cells. IC50 value is 4.8 µM, 11.41 µM, and 11.07 µM respectively. While complex-3 assessed against SH-SY5Y cancer cells since this complex shows greater effectivity against the SH-SY5Y cell line hence we are reporting IC_{50} value of this complex on neuroblastoma cancer cells which is 10.8 µM. Comparative study with cis platin is also reported.

Table 3b.14. Percent inhibition (IC_{50} values) of complex-3 and complex-4 against NCI-H23, SH-SY5Y and HepG2 Cells

Percent inhibition (IC_{50} values)			
Compounds	**Complex-3**	**Complex-4**	**Cisplatin**
NCI-H23	4.8 µM	-	17.65 µM
SH-SY5Y	11.41 µM	10.8 µM	44.94 µM
HepG2	11.07 µM	-	-

3b.2.8.1. Cell death analysis & Scratch assay

Cell death analysis provides a count of both live and dead cells using calcein and EthD-1 dyes which is responsible for green fluorescence (indicates live cells) and red fluorescence (indicates dead cells) respectively. The results demonstrate that complex-**3** is more effective against NCI-H23 cells. The scratch assay is a straightforward and economical method to study cell migration *in vitro*. It has been examined at three different times interval : at 0 h, 24 h and 48 h. At 24 h to determine the rate of cell migration. After 24 h, treated cells showed 26% wound closure, compared to 41% in the control group. By 48 h, wound closure reached 75% in treated cells and 40% in the untreated group. A complex-**3** has significantly inhibits the migratory ability of NCI-H23 lung cancer cells.

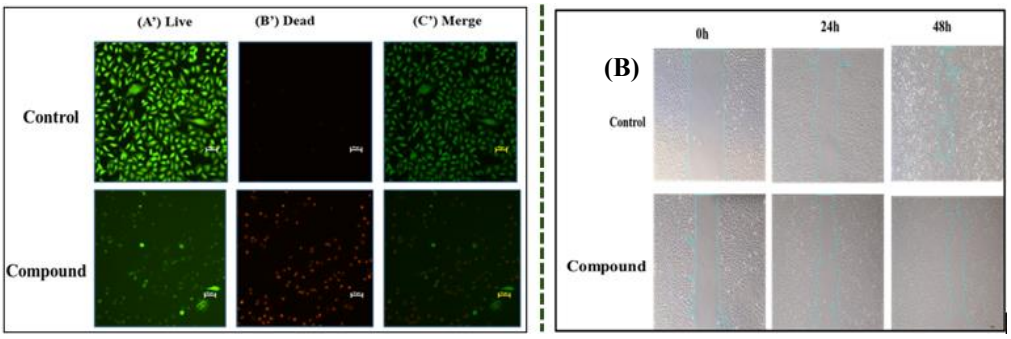

Fig.3b.8. (A) Dual staining (live/dead assay) of NCI-H23 cells exposed to complex-3, (B) Scratch assay

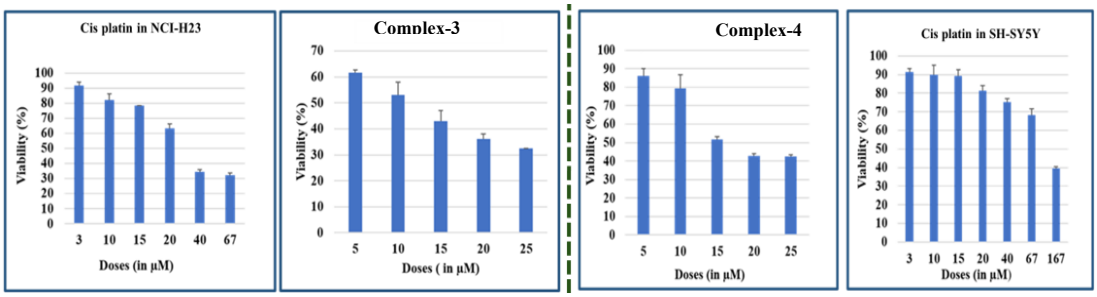

Fig.3b.9. (i)Percent viability of NCI-H23 Cells exposed to indicated doses of Cisplatin & complex-2
(ii) Percent viability of NCI-H23 Cells exposed to indicated doses of Cisplatin and complex-3

Conclusion

The design and synthesis of pyrazoles is a promising topic of research since they are an important pharmacophore with a diversity of biological characteristics. In this research we discussed the synthesis and characterization of complex-**3** & complex-**4**. Square Pyramidal geometry of the stable copper complexes demonstrated by single crystal X-ray crystallography. B3LYP/6-31G and B3LYP/LANL2DZ two different

basis set were used to optimized both complexes. *In vitro* anticancer activity indicates the positive application of the complex. We found that lung cancer cells' ability to survive and spread can be inhibited by the complex-**3**.

Chapter 4; Synthesis of New Square planar Cu(II) complexes derived from acylpyrazolone ligand: Molecular structure Computational, Hirshfeld analysis and antiproliferative properties

Part (a): Cytotoxicity assay and gene expression studies of acylpyrazolone-based square planar Cu(II) complexes: synthesis, characterization and computations

Experimental work

Synthetic route of complex-4 & complex-5

Both copper complexes, complex-**4** and complex-**5**, were prepared using the same procedure outlined in Chapter **3a.**

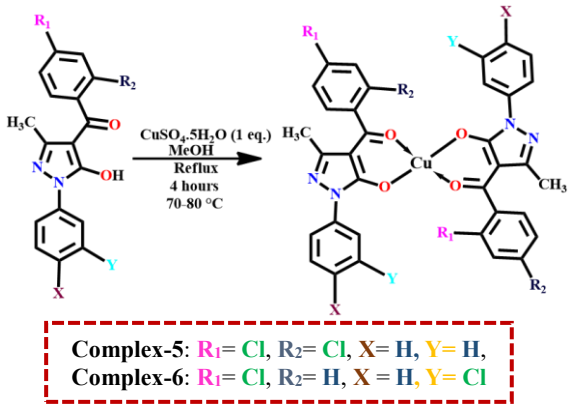

Fig.4a.1. Synthetic route of complex-4 and complex-5

Complex-5: yield: 85%, **Molecular formula:** $C_{34}H_{22}Cl_4CuN_4O_4$, **M.W**: 755.921, Elemental analysis: C (Exp. 53.92%, Calc. 54.02%); H (Exp. 2.90%, Calc. 2.93%); N (Exp. 6.96%, Calc. 7.41%); Cu (Exp. 8.10%, Calc. 8.08%), **FTIR (KBr, cm^{-1}):** ν(C=O) of pyrazolone: (1602), ν(C=O) of 2,4-dichloro benzoyl chloride: (1577), cyclic ν(C=N): (1435), **Molar conductance (10^{-3} M DMF):** 3.27 ohm^{-1}cm^{2}mol^{-1}.

Complex-6: yield: 86%, **Molecular formula:** $C_{38}H_{36}Cl_2N_5NiO_6$, **M.W:** 788.32, gravimetrically and volumetrically, Elemental analysis: C (Exp. 49.20%, Calc. 49.49%); H (Exp. 3.03%, Calc. 3.03%); N (Exp. 7.50%, Calc. 7.80%); Cu (Exp. 8.07%, Calc. 8.05%), (Metal estimation- gravimetrically and volumetrically), **FTIR (KBr, cm^{-1}):** ν(C=O) of pyrazolone: (1601), ν(C=O) of 2,4-dichloro benzoyl chloride: (1586), cyclic ν(C=N): (1475), **Molar conductance (10^{-3} M DMF):** 2.18 ohm^{-1}cm^{2}mol^{-1}.

Results and discussion

FTIR spectral studies

Table 4a.1. FTIR spectral data of respective ligands, complexe-5 and complex-6

Code	HL^I ligand	Complex-5	HL^V ligand	Complex-6
ν(C=O) of benzoyl chloride	1587	1577	1590	1586
ν(C=O) of Pyrazolone	1627	1602	1625	1601
Cyclic ν(C=N)	1515	1435	1551	1475
C–H in plane deformation	1394	1379	1385	1360
ν_{M-O}	-	508	-	490

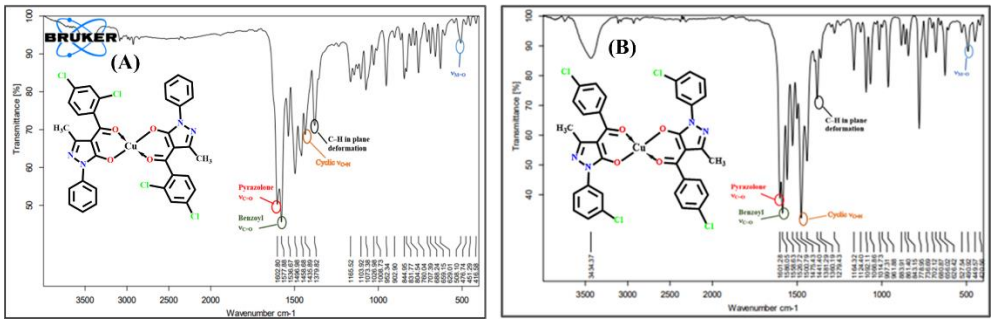

Fig.4a.2. FTIR spectra of (A) complex-5 & (B) complex-6

Thermogravimetric analysis

The copper complex thermally decomposes between 100 and 550°C, demonstrating the remarkable thermal stability of complex. Degradation of ligand moiety is 76.5% and 63.5% in complex-4 and complex-5 respectively.

Single crystal X-ray diffraction study

$[Cu(HL^{I})_2]$ complex-5: α= 90.834(4)°, β= 95.017(4)°, γ=106.124(4)°, a = 9.6075(12)Å, b= 11.7452(15)Å, c= 14.3696(17)Å, Triclinic space group *P*-1.

$[Cu(HL^{V})_2]$ complex-6: = 90°, β= 111.660(4)°, γ=90°, a = 9.0930(11)Å, b= 27.412(3)Å, c= 6.8238(8)Å, Monoclinic space group $P2_1/c$.

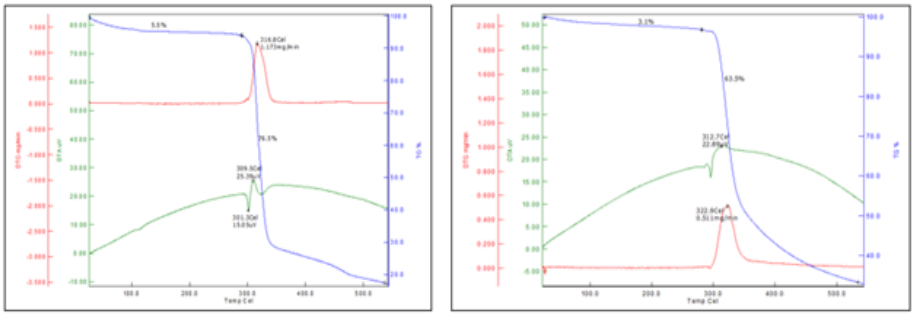

Fig.4a.3. TG-DTA plot of complex-5 & complex-6

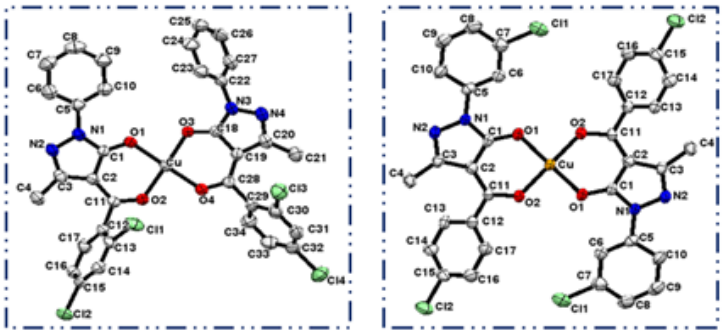

Fig.4a.4. ORTEP view of $[Cu(HL^{I})_2]$ complex-5 & $[Cu(HL^{V})_2]$ complex-6

DFT based computational analysis & Hirshfeld surface area analysis

The geometry optimization of complex-**5** and complex-**6** were done via B3LYP/6-31G level basis set using Gauss View 6.0 software. The energy value of complex-**5** and complex-**6** are -144.475 keV, -144.475 keV. HOMO-LUMO energies play an essential role to determine a variety of chemical interaction.

With the help of Crystal Explorer 17.5 program, the donor-acceptor interaction sites and intermolecular contacts can be visualized in this analysis 3D Hirshfeld surfaces have been mapped over dnorm, de, di, shape index, curvedness and fragment patch.

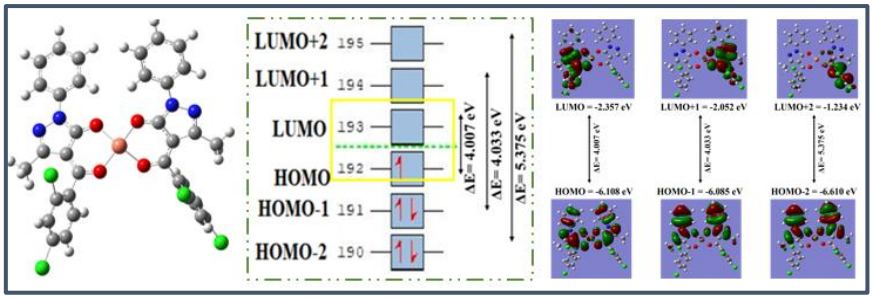

Fig.4a.4. DFT optimized geometry & HOMO-LUMO orbital of complex-5

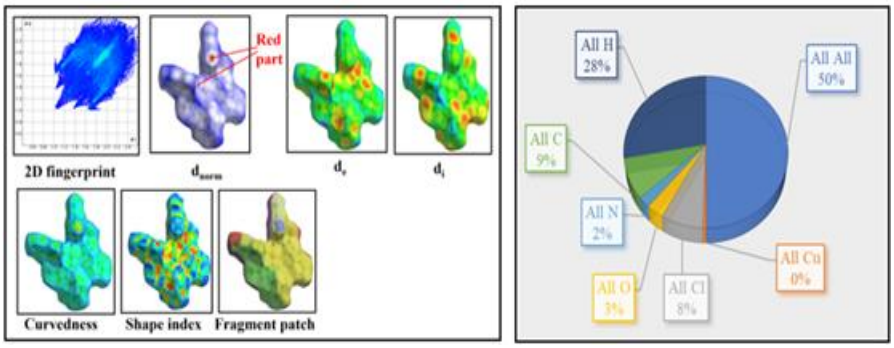

Fig.4a.5. Molecular hirshfeld diagram of complex-5

Electronic spectral analysis

The electronic spectra of Square Planar complex-4 and complex-5 were recorded in a DMSO. The crystal sample underwent UV-visible absorption investigations up to 950 nm to determine the energy gap of copper complexes. DMSO solvent was used for the analysis. The particular transition occurs from the $^2E_g \rightarrow {}^2T_{2g}$ transition.

Complex-4: π-π*(277 nm), n-π*(333 nm), d-d transition (742 nm)

Complex-5: π-π*(283 nm), n-π*(352 nm), d-d transition (739 nm)

ESR & Electro chemical analysis

The ESR spectral analysis of two copper complexes was carried out using ESR JEOL analysis in powder state at RT and in solution state at LNT. The value of $g_{\|}$ for complex-**5** and complex-**6** is found to be 2.370 (RT), 2.370 (LNT) and 2.204 (RT), 2.313 (LNT), respectively, and the value for $g_{\perp}$ is found to be 2.063, 2.052 for complex-5 and complex-6, respectively. The g tensor values, where $g_{\|} > g_{\perp} > 2.0023$ indicate the presence of an unpaired electron in a $dx^2\text{-}y^2$ orbital. The redox behaviour of both complexes studied through cyclic voltammetry (CV) technique. The ratio of the first anodic to cathodic peak current (Ipa_1/Ipc_1) for complex-5 is -0.0046 amp and for the second peak (Ipa_2/Ipc_2) is -2.4671 amp. For complex-6, the (Ipa_1/Ipc_1) ratio is -0.0047 amp and (Ipa_2/Ipc_2) ratio is -2.1788 amp.

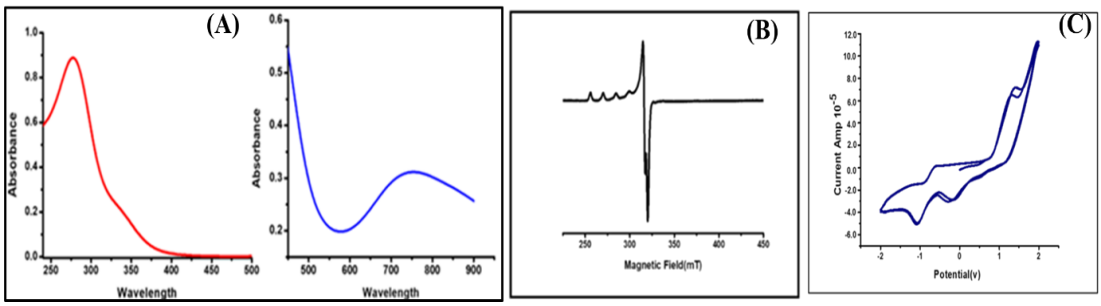

Fig.4a.6. Complex-5: (A) Electronic spectra, (B) ESR spectrum at LNT, (C) CV plot

Cytotoxicity assay

Cell viability was assessed using an MTT assay. The copper complexes were able to inhibit the cell viability of NCI-H23, SH-SY5Y and HepG2 cancer cells. IC50 was calculated against Cisplatin on SH-SY5Y neuroblastoma cancer cell line. The IC50 value is 44.94µM for cisplatin. Complex-5 gave the best result against SH-SY5Y cell line. Hence further study has been done on a complex-5. Such as Live/dead assay and Gene expression study by qRT-PCR against BAD and BCL2L1 genes. IC_{50} value for complex-4 is 7.2 µM, 12.3 µM, and 9.0 µM and complex-5 was reported to 8.4 µM, 8.4 µM, and 10.7 µM against NCI-H23, SH-SY5Y, and HepG2 cells respectively.

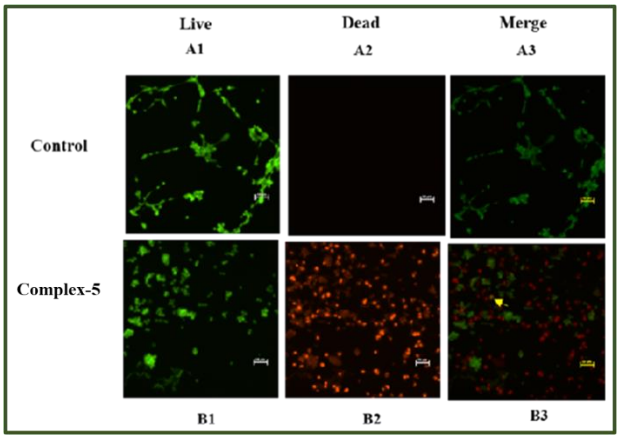

Fig.4a.7. Live/dead assay of SH-SY5Y cells exposed to complex-6

Conclusions

The formation of two copper (II) complexes based on acyl pyrazolone ligand has been done and characterized. The geometry around copper center is square planar proved by X-ray crystallography technique. Both complexes were optimized via DFT/B3LYP/6-31G method. ESR study suggested the paramagnetic behaviour of complex. To study the intermolecular interactions Hirshfeld surface analysis was employed. *In vitro* anticancer activity suggesting the encouraging application of both the complexes.

Part (b): Two New Square Planar Cu(II) complexes derived from a heterocyclic Pyrazolone ligand: Synthesis, *in vitro* anticancer activity, DFT and Hirshfeld analysis

Experimental work

Synthetic route of complex-6 & complex-7

Both copper complexes, complex-**4** and complex-**5**, were prepared using the same procedure outlined in Chapter **3a.**

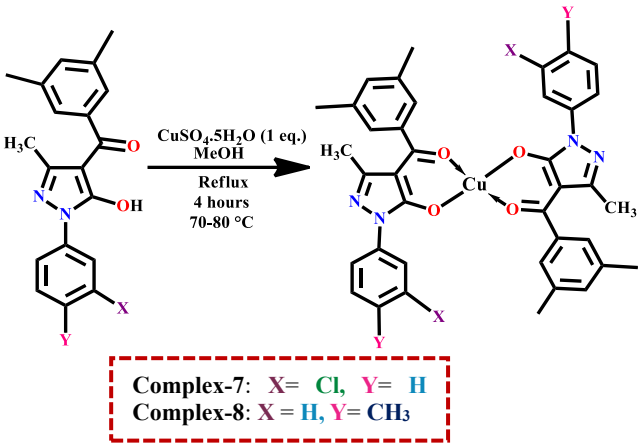

Fig.4b.1. Synthetic route of complex-7 and complex-8

Complex-7 : **Colour**: Green, yield: 82%, M.P:> 200°C, Molecular formula: $C_{38}H_{32}CuCl_2N_4O_4$, M.W: 743.14, **Elemental analysis**: C (Exp. 60.97%, Calc.: 61.42%); H (Exp. 4.86%, Calc. 4.34%); N (Exp. 8.23%, Calc. 7.54%); Cu = 8.03 %, **FTIR(KBr, cm^{-1}):** 1585 ($\nu_{C=O}$ of pyrazolone), 1603 ($\nu_{C=O}$ of 3,5-dimethyl benzoyl), 1485 ($\nu_{C=N}$), 596 ($\nu_{Cu=O}$), **Molar conductance(10^{-3} M DMF):** 4.0 ohm^{-1}cm^{2}mol^{-1}.

Complex-8 : **Colour**: Yellowish green, yield: 80 %, M.P: >200°C, Molecular formula: $C_{40}H_{38}CuN_4O_4$, M.W: 702.30, **Elemental analysis**: C (Exp. 67.95%, Calc.: 68.41%); H (Exp. 4.98%, Calc. 5.45%); N (Exp. 6.90%, Calc. 7.98%); Cu = 8.00%, **FTIR(KBr, cm^{-1}):** 1526 ($\nu_{C=O}$ of pyrazolone), 1593 ($\nu_{C=O}$ of benzoyl), 1492 ($\nu_{C=N}$), 513 ($\nu_{Cu=O}$), **Molar conductance(10^{-3} M DMF):** 4.5 ohm^{-1}cm^{2}mol^{-1}.

Results and discussion

FTIR spectral studies

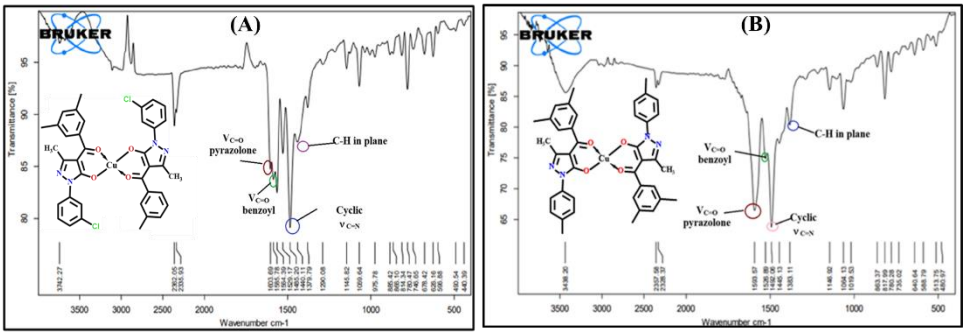

Fig.4b.2. FTIR spectra of (A) complex-7 & (B) complex-8

Thermogravimetric analysis

The mass loss and thermal stability of the material are inferred via thermogravimetric analysis (TGA). Thermal breakdown of the copper at temperatures around 100 and 550 °C demonstrates the remarkable thermal stability of both complexes. TGA analysis of the complex-**7** & complex-**8** revealed a total weight loss of 61.8% ,49.64% on TG graph respectively.

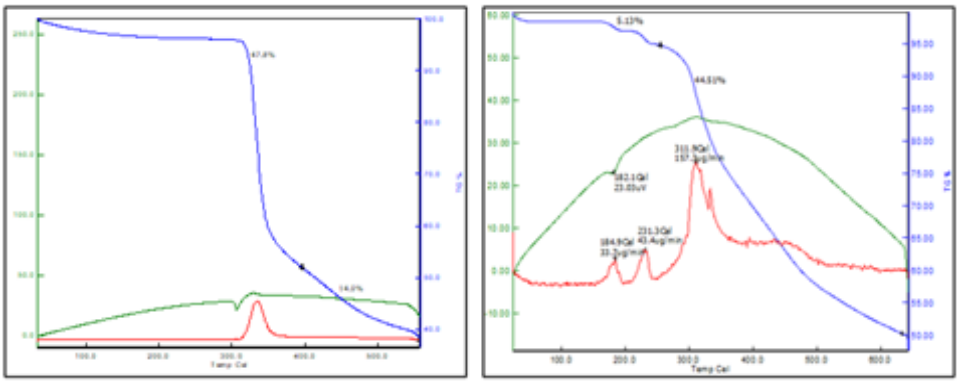

Fig.4b.3. TG-DTA plot of complex-6 & complex-7

Single crystal X-ray diffraction study

A geometry of the synthesized complexes appeared in the form of a Square Planner (Tetra coordinated) by the single crystal analysis. Cu-O bond length in both the complexes is 180 A°. The bond distance between Cu-O(1) in complex-6 & complex-7 is 1.917(12) Å and 1.910(19) Å respectively.

[Cu(HL^{VII})$_2$] complex-6: Z= 2, α= 90°, β= 97.8400(10)°, γ= 90°, a = 8.4243(2)Å, b= 27.7723(4)Å, c= 7.01630(10)Å, Monoclinic, $P2_1/c$ space group.

[Cu(HL^{VIII})$_2$] complex-7: Z= 2, α= 90°, β= 98.035(4)°, γ=90°, a = 7.2657(3)Å, b= 13.4359(4)Å, c= 18.2180(8)Å, Monoclinic, $P2_1/n$ space group.

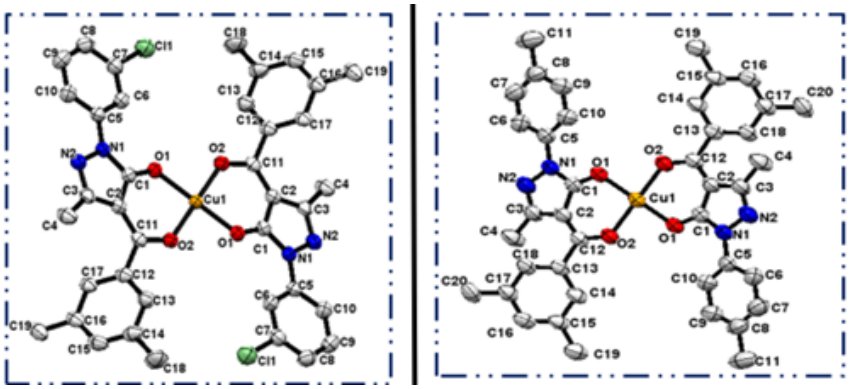

Fig.4b.4. ORTEP view of complex-7 and complex-8

DFT based computational analysis & Hirshfeld surface area analysis

The geometries were computed using B3LYP/LANL2DZ levels for both complexes. The optimization energy -123.7430 keV and -100.8708 keV respectively were observed for complex-**7** & complex-**8.**

Electronic spectral analysis

The crystal sample underwent UV-visible absorption investigations up to 950 nm to determine the energy gap of copper complexes. DMSO solvent was used for the analysis.

Complex-6: π-π*(282 nm), n-π*(358 nm), d-d transition (705 nm), Molar absorbance (ε): 36.9 M^{-1} cm^{-1}

Complex-7: π-π*(278 nm), n-π*(375 nm), d-d transition (706 nm) Molar absorbance (ε): 36.9 M^{-1} cm^{-1}

Spin density plot & NBO analysis

Natural Bond Orbital (NBO) analysis is a useful technique for the chemical interpretation of hyperconjugative interaction and electron density transfer from the filled lone pair electron. Cu^{+2} has 1.1676 natural atomic charges in complex-**8** and 1.1638 in complex-**7**. The natural electrical arrangement of a copper in both the complexes is [core] 3d (9.13) 4s (0.34) 4p (0.36). Spin densities may be calculated more informatively when an unpaired electron is present in the system. electronic spin density is positive and scattered over the metal centre while in regions where electrons are more likely to be found in the β spin state, it is negative

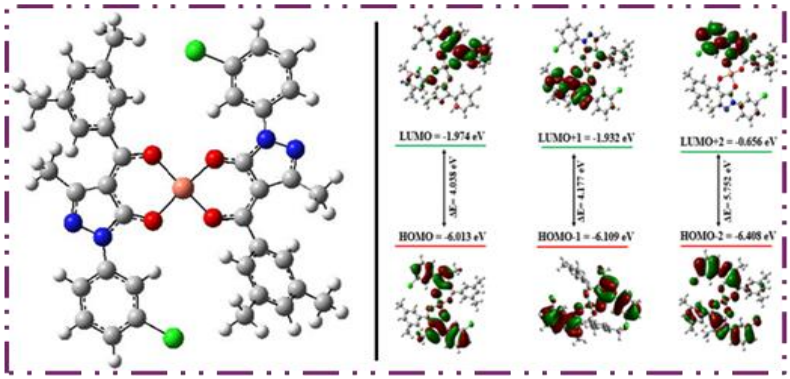

Fig.4b.5. DFT optimized geometry & HOMO-LUMO orbital of complex-7

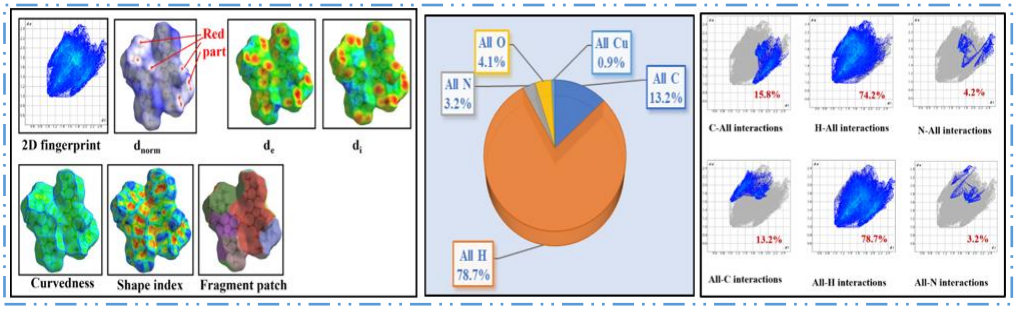

Fig.4b.6. Fig.4.18. Molecular hirshfeld diagram & 2d fingerprint plot of complex-8

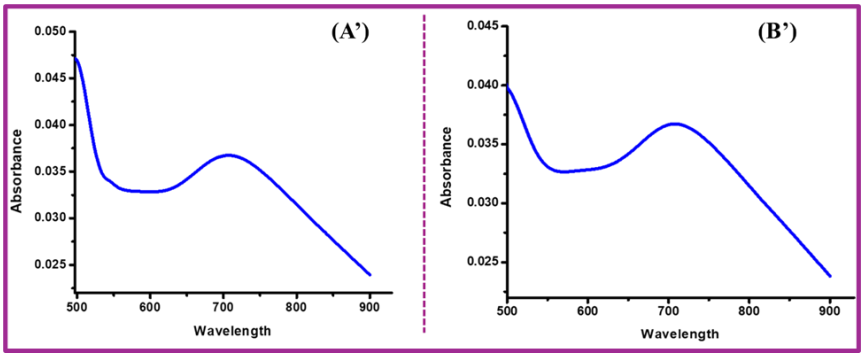

Fig.4a.7. d-d transition observed in complex-7 and complex-8

ESR & Electro chemical analysis

The value of $g_{\parallel}$ at LNT is found to be 2.3562, and $g_{\perp}$ is 2.0690. The value of g tensor is $g_{\parallel} > g_{\perp} > 2.0023$ supports the Square Planner geometry. A geometric parameter G value is found to be 5.1623 by this formula $G = (g_{\parallel} - 2.0023)/(g_{\perp} - 2.0023)$.

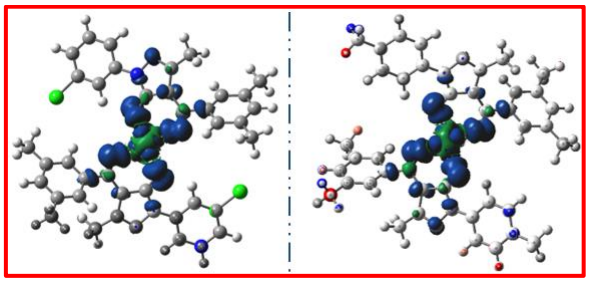

Fig.4b.8. Spin density plot of complex-7 & complex-8 respectively

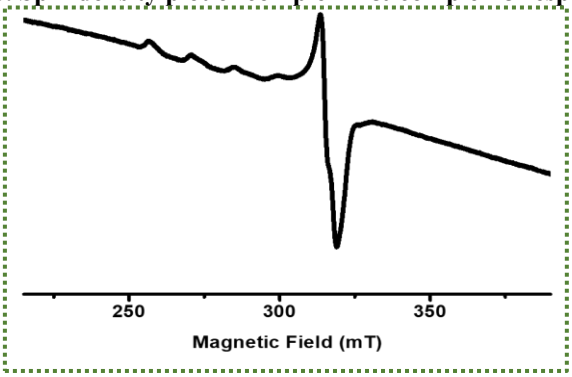

Fig.4b.9. X-band ESR spectra of in the solution state at LNT

4b.2.8. Cytotoxicity assay

Cell viability was assessed by MTT assay. Three different cancer cell lines were used against complex-**8** to check an antiproliferative activity. As per the analysis complex-7 gave the best result on SH-SY5Y(Neuroblastoma cancer cells) because of its lower IC50 value (3.9 µM). IC50 value of cis platin was recorded 44.9 µM, this surpasses the complex's IC50 value. The outcomes indicate that the synthesized copper complex is more effective than cisplatin.

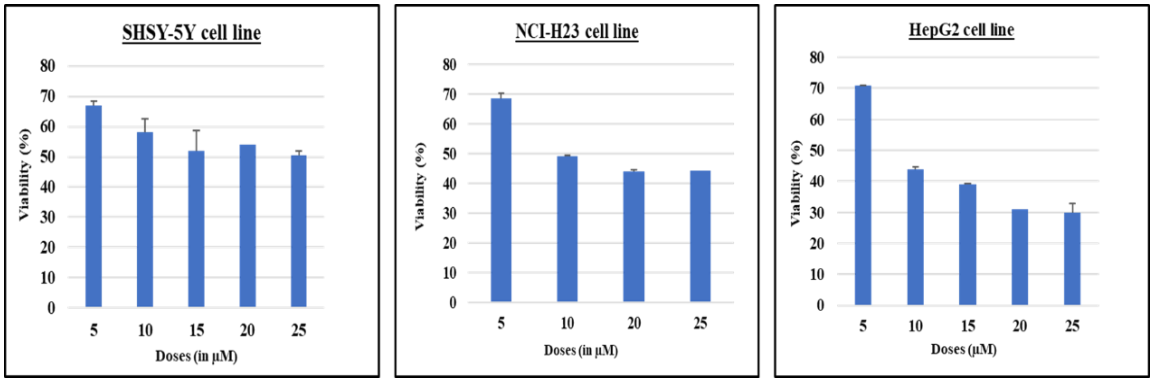

Fig.4b.10 Percent viability of NCI-H23, SH-SY5Y and HepG2 Cells exposed to indicated doses of complex-8

Conclusion

We successfully investigated new Copper(II) complexes with square planar geometry. A variety of analytical techniques were employed for the characterization. The computational study of the synthesized compounds was studied using B3LYP/LanL2DZ basis set and the HOMO-LUMO energy gap was calculated. X band ESR measurement at LNT was used to establish the complexes' magnetic properties. Lower IC_{50} value inspired the complex to compare with the well-known drug Cis platin against SH-SY5Y cancer cells.

Chapter 5; Chemical assessment of three Octahedral Ni(II) Complexes with heterocyclic Acylpyrazolone ligand: Crystal structure, DFT-NBO analysis, Hirshfeld and Magnetic study

Experimental work

Synthetic route of complexes 9,10 &11

Hot ethanolic solution of HL^{VIII} ligand, HL^{IV} ligand and HL^{VI} ligand and Nickel metal salt were taken in three different round-bottom flasks attached to water condenser. The resulting mixture was refluxed for eight to ten hours at 70-80°C temperature in three separate round-bottom flasks. After Reflux, Pale green precipitates of all three synthesized Nickel complexes were produced. HL^{VIII}, HL^{IV}, HL^{VI} all three ligands have already been reported in the previously published articles by our lab. **HL^{VIII} ligand** (0.6403g, 0.002 mol), **HL^{IV} ligand** (0.625g, 0.002 mol), **HL^{VI} ligand** (0.653g, 0.002 mol).

Complex-9: Pale bluish green crystal, yield: 81%, Molecular formula (crystal structure): $C_{44}H_{50}N_4NiO_6$, **M.W**: 789.58, **Elemental analysis**: C (Exp. 65.39%, Calc. 66.9%); H (Exp. 6.3%, Calc. 6.3%); N (Exp. 8.23%, Calc. 7.54%); Ni = 8.4% (Metal estimation- gravimetrically and volumetrically), **FTIR(KBr, cm^{-1}):** ν(C=O) of pyrazolone: (1602), ν(C=O) of benzoyl chloride: (1540), cyclic ν(C=N): (1486)

Complex-10: Pale green crystal, yield: 81%, Molecular formula (crystal structure): $C_{38}H_{36}Cl_2N_5NiO_6$, **M.W**: 788.32, **Elemental analysis**: C (Exp. 57.39%, Calc. 58.10%); H (Exp. 4.20%, Calc. 4.60%); N (Exp. 8.23%, Calc. 8.88%); Ni = 8.6% (Metal estimation- gravimetrically and volumetrically), **FTIR(KBr, cm^{-1}):** ν(C=O) of pyrazolone: (1668), ν(C=O) of benzoyl chloride: (1585), cyclic ν(C=N): (1472).

Complex-11: Pale yellow-green crystal, yield: 83%, **Molecular formula** (crystal structure): $C_{42}H_{46}Cl_2N_4NiO_6S_2$, **M.W**: 896.57, **Elemental analysis**: C (Exp. 55.92%, Calc.: 56.26%); H (Exp. 5.10%, Calc. 5.15%); N (Exp. 6.10%, Calc. 6.25%); Ni = 8.4% (Metal estimation gravimetrically and volumetrically), **FTIR(KBr, cm^{-1}):** ν(C=O) of pyrazolone: (1613), ν(C=O) of benzoyl chloride: (1590), cyclic ν(C=N): (1457).

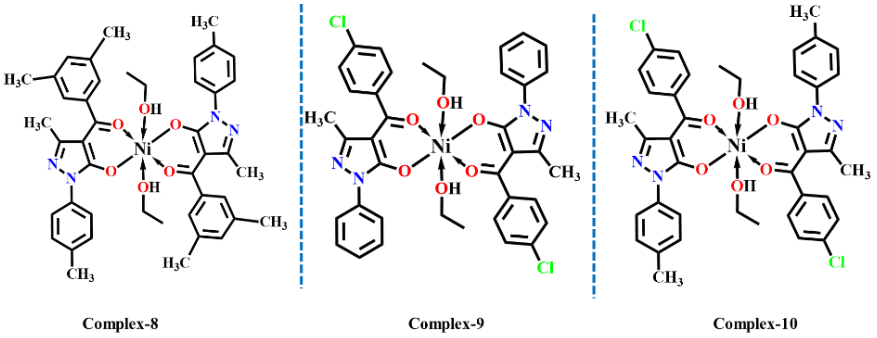

Fig.5.1. Structure of complexes 9, 10 and 11

Results and discussion

FTIR spectral studies and Thermogravimetric analysis

All the synthesized Nickel complexes are octahedral. TGA, describes how the mass of a substance changes as a function of temperature. Thermal breakdown at temperatures between 100 and 550 °C serves as evidence of the remarkable thermal stability of the three synthesized Ni(II) complexes.

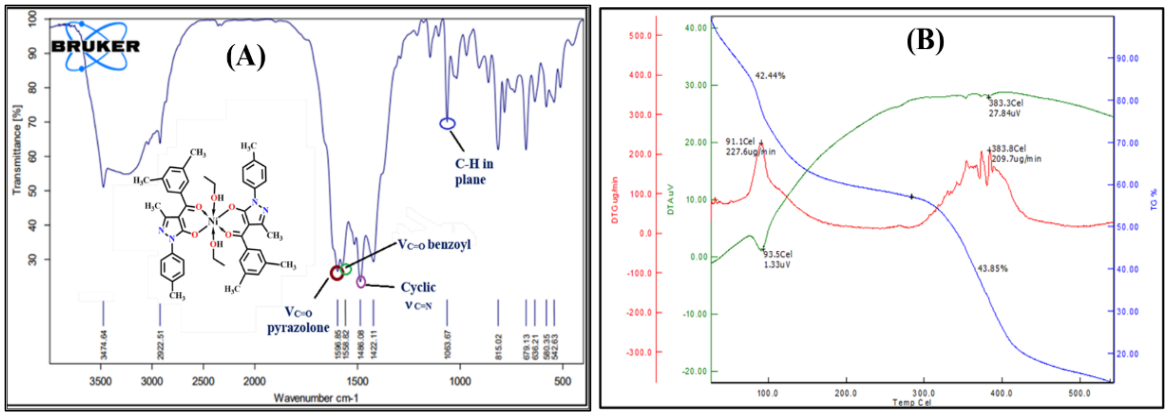

Fig.5.2. Complex-9: FTIR spectra of (A) FTIR spectrum and (B) TGA spectrum

Single crystal X-ray diffraction study and Powder XRD analysis

The structural analysis evidenced that the Ni centre is "octahedrally coordinated" from each six oxygen atoms in three complexes. Complex-**9** and complex-**10** crystallize in a 'Triclinic crystal system' with space group *P*-1 while complex-**11** crystallizes in a 'Monoclinic crystal system' with space group $P2_1/n$.

In the XRD graph, a sharp band is observed with maxima 2θ = 5 to 25° range for complex-10. The simulated pattern matches well with the experimental pattern which confirms a similar geometry of the complexes. This also ensures the structure obtained from a single crystal represents the bulk of the complexes.

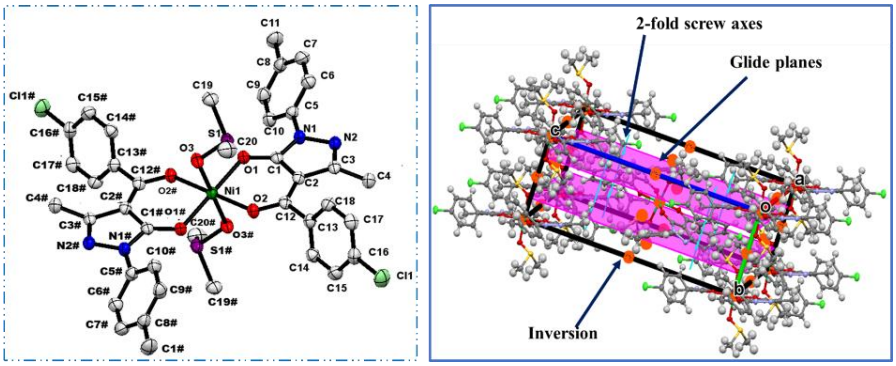

Fig.5.3. ORTEP view and symmetry elements of complex-11

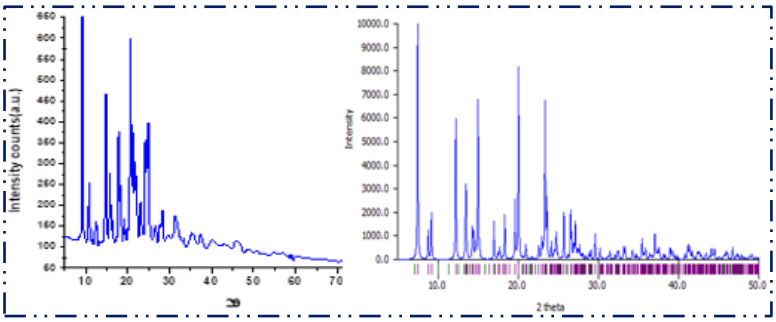

Fig.5.4. Experimental & Simulated powder XRD pattern of complex-11

Electronic spectral analysis and Magnetic study

Electronic transition(d-d spectra) of complex-9 and complex-11 were obtained in a 100% DMSO (1×10^{-3} M) solution up to 950 nm. While d-d bands of complex-10 were obtained in 10^{-2} M concentration. **Table 5.1. Band Assignments of all three Ni(II) complexes**

	Complex-9	Complex-10	Complex-11
$3A_{2g}\rightarrow3T_{1g}(P)$	516 nm, (1.7 $M^{-1}cm^{-1}$)	502 nm, (2.0 $M^{-1}cm^{-1}$)	773 nm, (0.3 $M^{-1}cm^{-1}$)
$3A_{2g}\rightarrow3T_{1g}(F)$	652 nm, (4.0 $M^{-1}cm^{-1}$)	669 nm, (3.8 $M^{-1}cm^{-1}$)	752 nm, (1.7 $M^{-1}cm^{-1}$)
$3A_{2g}\rightarrow3T_{2g}$	773 nm, (0.3 $M^{-1}cm^{-1}$)	652 nm, (3.0 $M^{-1}cm^{-1}$)	770 nm, (0.5 $M^{-1}cm^{-1}$)

A superconducting quantum interference (SQUID) device is used to study a material's magnetic characteristics at different magnetic fields and temperatures. Temperature-dependent magnetisation data at 500 Oe (0.05T) was obtained using SQUID. According to Curie–Weiss paramagnetism, Magnetic susceptibility is inversely proportional to temperature hence, by increasing temperature the susceptibility decreases.

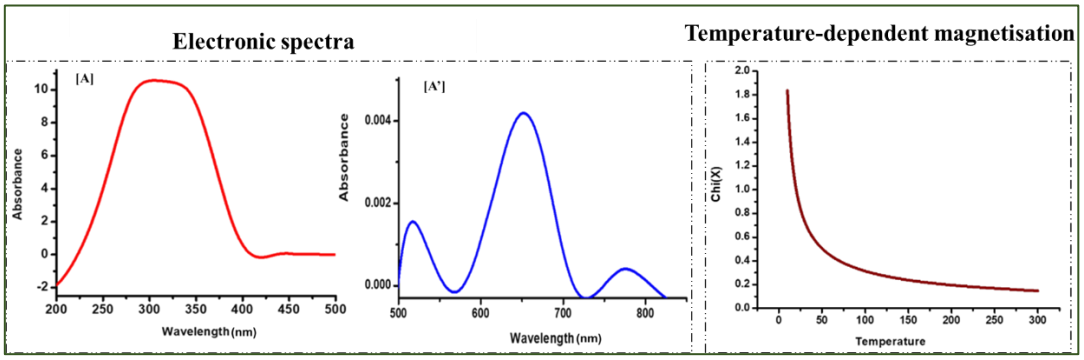

Fig.5.5. Electronic spectra and magnetization graph

DFT based computational analysis & Hirshfeld surface area analysis

The geometry of all three Ni(II) complexes were optimized via B3LYP/LANL2DZ level basis set using Gauss View 6.0 software. The optimization energy is -105.7622 keV, -64.0523 keV and -66.3350 keV of complex-**9,10 and 11**, respectively.

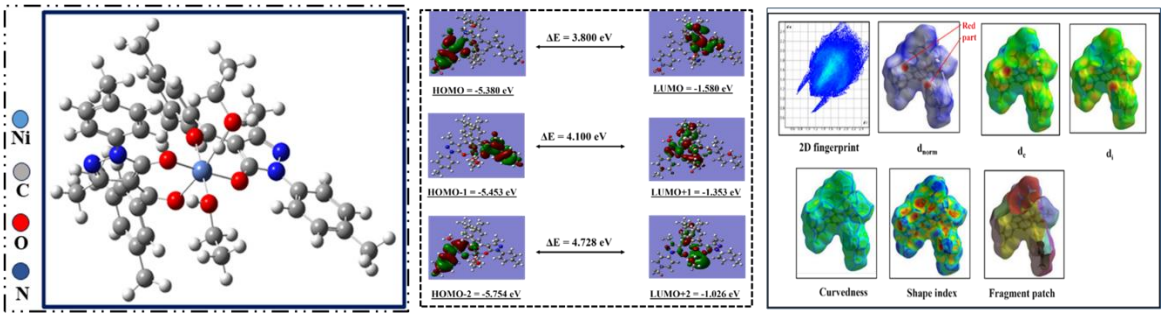

Fig.5.6. DFT optimized geometry, HOMO-LUMO orbitals and Hirshfeld diagram of complex-9

Conclusion

Acylpyrazolone based three Ni(II) complexes were synthesized having Octahedral geometry. All three complexes were characterized using analytical method. X-ray single-crystal diffraction data reveals that the ligand coupled to Ni(II) ions in all three complexes via O donor atoms. Magnetic study revealed the paramagnetic nature of the complexes. Multiple interactions have been identified through Hirshfeld surface analysis. DFT and HOMO-LUMO study were conducted. The magnetic study revealed the paramagnetic nature of complexes.

References

[1] F. Marchetti, C. Pettin ari, R. Pettinari, Acylpyrazolone ligands: Synthesis, structures, metal coordination chemistry and applications, Coord. Chem. Rev. 249 (2005) 2909–2945. https://doi.org/10.1016/j.ccr.2005.03.013.

[2] F. Marchetti, R. Pettinari, C. Pettinari, Recent advances in acylpyrazolone metal complexes and their potential applications, Coord. Chem. Rev. 303 (2015) 1–31. https://doi.org/10.1016/j.ccr.2015.05.003.

[3] F. Marchetti, C. Pettinari, C. Di Nicola, A. Tombesi, R. Pettinari, Coordination chemistry of pyrazolone-based ligands and applications of their metal complexes, Coord. Chem. Rev. 401 (2019) 213069. https://doi.org/10.1016/j.ccr.2019.213069.

[4] B.S. Jensen, H. Meier, K. Lundquist, S. Refn, The Synthesis of 1-Phenyl-3-methyl-4-acyl-pyrazolones-5., Acta Chem. Scand. 13 (1959) 1668–1670. https://doi.org/10.3891/acta.chem.scand.13-1668.

[5] E.C. Okafor, The metal complexes of heterocyclic β-diketones and their derivatives-VI. The synthesis, structure and i.r. spectral studies of some new metal(II) complexes of 1-phenyl-3-methyl-4-benzoyl-pyrazolone-5 (HPMBP), Spectrochim. Acta Part A Mol. Spectrosc. 37 (1981) 945–950. https://doi.org/10.1016/0584-8539(81)80020-7.

[6] C. Molinaro, A. Martoriati, L. Pelinski, K. Cailliau, Copper Complexes as Anticancer Agents Targeting, (2020) 1–27.

[7] R.N. Jadeja, S. Parihar, K. Vyas, V.K. Gupta, Synthesis and crystal structure of a series of pyrazolone based Schiff base ligands and DNA binding studies of their copper complexes, J. Mol. Struct. 1013 (2012) 86–94. https://doi.org/10.1016/j.molstruc.2012.01.006.

[9] F.K. Keter, J. Darkwa, Perspective: The potential of pyrazole-based compounds in medicine, BioMetals. 25 (2012) 9–21. https://doi.org/10.1007/s10534-011-9496-4.

[9] P.J. Hay, W.R. Wadt, Ab initio effective core potentials for molecular calculations. Potentials for the transition metal atoms Sc to Hg, J. Chem. Phys. 82 (1985) 270–283. https://doi.org/10.1063/1.448799.

[10] M. Travadi, R.N. Jadeja, R.J. Butcher, Synthesis, Covalency Sequence, and Crystal Features of Pentagonal Uranyl Acylpyrazolone Complexes along with DFT Calculation and Hirshfeld Analysis, ACS Omega. 7 (2022) 34359–34369. https://doi.org/10.1021/acsomega.2c03923.

[11] G.M. Sheldrick, SHELXT - Integrated space-group and crystal-structure determination, Acta Crystallogr. Sect. A Found. Crystallogr. 71 (2015) 3–8. https://doi.org/10.1107/S2053273314026370.

[12] G. Vala, A.A. Puranik, R.N. Jadeja, D. Choquesillo-Lazarte, Solvent Free, Selective Oxidation of Styrene Catalyzed by Cobalt Acylpyrazolone Supported onto Neutral Alumina: Synthesis and Spectral Characterization, ChemistrySelect. 9 (2024). https://doi.org/10.1002/slct.202304086.

[13] I.U. Shaikh, Synthesis , Characterization and Studies on d 10 Metal Complexes derived from Acyl Pyrazolones, (2020).

[14] M. Travadi, R.N. Jadeja, R.J. Butcher, M.S. Shekhawat, Neodymium based acylpyrazolone complexes: Synthesis and physicochemical characterizations, Inorganica Chim. Acta. 559 (2024) 121766. https://doi.org/https://doi.org/10.1016/j.ica.2023.121766.

[15] S.P.C. Cole, Rapid chemosensitivity testing of human lung tumor cells using the MTT assay, Cancer Chemother. Pharmacol. 17 (1986) 259–263. https://doi.org/10.1007/BF00256695.

Research publications

1. S. Barad, K. Chaudhari, R.N. Jadeja, H. Roy, D. Choquesillo-Lazarte, Square pyramidal Cu(II) acylpyrazolone complex: Synthesis, characterization, crystal structure, DFT and Hirshfeld analysis, in-vitro anti-cancer evaluation, J. Mol. Struct. 1294 (2023) 136345. https://doi.org/10.1016/j.molstruc.2023.136345.

2. S. Barad, K. Chaudhari, H. Roy, R.J. Butcher, R.N. Jadeja, Acylpyrazolone based squarepyramidal Cu(II) complexes: Synthesis, structural characterization, DFT and antiproliferative properties, Inorganica Chim. Acta. 559 (2024) 121794. https://doi.org/10.1016/j.ica.2023.121794.

3. S. Barad, K. Chaudhari, R.N. Jadeja, H. Roy, R.J. Butcher, Cytotoxicity assay and gene expression studies of acylpyrazolone-based square planar Cu(II) complexes: synthesis, characterization and computations, J. Coord. Chem. 76 (2023) 1955–1983. https://doi.org/10.1080/00958972.2023.2289004.

4. S. V. Barad, S. Saurabhb, D. Choquesillo-Lazarte, R.N. Jadeja, Chemical assessment of three octahedral Ni(II) complexes with heterocyclic acylpyrazolone ligand: Crystal structure, DFT-NBO analysis, Hirshfeld and Magnetic study J. Mol. Struct. 1321 (2025) 140213. https://doi.org/10.1016/j.molstruc.2024.140213.

5. S.V. Barad, R.N. Jadeja, R.J. Butcher, Crystal structure, DFT and Hirshfeld surface analysis of acylpyrazolone based square pyramidal Copper(II) complex: *In-vitro* anticanceractivity, Inorganica Chim. Acta (Under review, MS no. ICA-D-24-01168).

6. S.V. Barad, R.N. Jadeja, R.J. Butcher, Two New Square Planar Cu(II) complexesderived from a heterocyclic Pyrazolone ligand: Synthesis, *in vitro* anticancer activity, DFT and Hirshfeld analysis (Communicated).

•••

Barad Sapnaben Vishnubhai
Research Scholar

24/10/25

Dr. R. N. Jadeja
Research Supervisor

Department of Chemistry,
Faculty of Science,
The Maharaja Sayajirao University of Baroda
Vadodara.-390002. GUJARAT- INDIA.

Prof. Ashutosh V. Bedekar
Offg. Head
Department of Chemistry

HEAD
Department of Chemistry
Faculty of Science
The Maharaja Sayajirao University of Baroda
Vadodara - 390002. Gujarat - INDIA